Colloid Polym Sci (2008) 286:545–551
DOI 10.1007/s00396-007-1799-1

ORIGINAL CONTRIBUTION

Solubilization of endocrine disruptors in micellar media

Osamu Kosaka · Shunsuke Iida · Pankaj Sehgal · Hidekazu Doe

Received: 19 June 2007 / Revised: 31 October 2007 / Accepted: 5 November 2007 / Published online: 28 November 2007

Abstract The interaction of endocrine disruptor chemicals (EDCs) such as nonylphenol (NP) and β-estradiol with cationic micelle of hexadecyltrimethylammonium ion (HTA^+) and a monolayer of HTA^+ ion adsorbed at the electrode surface has been investigated in the presence of hydrophilic modified (2-hydroxypropyl)-β-cyclodextrin. NP, which has a similar structure to HTA^+, decreased the critical micelle concentration (cmc) of hexadecyltrimethylammonium bromide more effectively. At the low HTA^+ concentration, HTA^+ inhibited the adsorption of I_2. However, as the HTA^+ concentration increased, a monolayer of HTA^+ was formed at the electrode surface and caused the adsorption of iodine molecule (I_2). In the presence of micelle, the I_2 was dissolved in the micelle. Both EDCs caused the formation of HTA^+ monolayer even at the HTA^+ concentration below the cmc.

Keywords Nonylphenol · β-Estradiol · Cyclodextrin · Surfactant · Micelle

Introduction

A wide variety of artificial chemicals are currently being released into the environment. Some of these chemicals have the potentiality to cause serious effects on wildlife and human health, even when they are present at very low concentrations over a period of time. Such effects include the apparent increase in hormone-dependent cancers and disorders of the reproductive tract in wildlife and humans [1–4]. Nonylphenol (NP) was known to be an endocrine disruptor. NP has a carbon chain and a phenolic group in its molecule structure. NP is used as a material of nonionic surfactant, nonylphenolethoxylate. Also, the degradation process of its surfactant sewage can release the suspicious NP into the environment. On the other hand, β-estradiol (β-E2) is a major estrogen and has the highest activity on our human body [5]. It is used in obstetric treatments. NP and β-E2 are observed in soil and water. In sewage water, a wide variety of surfactants can be found and coexist with those endocrine disruptor chemicals (EDCs). Therefore, it is very interesting to investigate the interaction between ionic surfactants and those endocrine disruptors.

We have investigated the interactions between ionic surfactants and bisphenol A (BPA) [6, 7]. In our previous paper, we observed the favorable interactions of BPA especially with cationic hexadecyltrimethylammonium bromide (HTAB). BPA decreased the amount of surfactant molecules absorbed at the air–solution interface where BPA adsorbs cooperatively with HTAB. BPA alone does not adsorb at the air–solution interface. Moreover, BPA stabilized the micelle formation and the adsorption of surfactant molecules at the air–solution interface, which was more significant at the air–solution interface, and enhanced the degree of micelle ionization [6]. In this paper, we have studied NP and β-E2. These EDCs are almost insoluble in water and the solubility of NP is reported to be 22 μM [8]. NP is surface active to some extent (41 mNm at a saturated aqueous solution) and β-E2 is not surface active. Their solubilities are too low in water to assess the interaction with surfactants and it is difficult to prepare the solutions of accurate concentrations. Therefore, we adopted (2-hydroxypropyl)-β-cyclodextrin (hp-β-CD) to enhance the solubility of NP [9]. Herein, we report the interactions

O. Kosaka (✉) · S. Iida · P. Sehgal · H. Doe
Department of Chemistry, Graduate School of Science,
Osaka City University,
3-3-138 Sugimoto, Sumiyoshi-ku,
Osaka 558-8585, Japan
e-mail: kosamu_2006@yahoo.co.jp

of the endocrine disruptors NP and β-E2 with HTAB in the presence of hp-β-CD and compare them with the interactions of BPA. In addition, we have measured the voltammetry of I_2/I^- as an electrochemical probe to investigate the behavior of NP and β-E2 in the hexadecyltrimethylammonium ion (HTA^+) monolayer formed at the platinum electrode surface. The electrochemical reaction of I_2/I^- is strongly affected by the condition of the HTA^+ monolayer on that electrode.

Experimental

Materials

Cationic surfactant HTAB (>98.0% pure) was purchased from Tokyo Kasei (Japan). NP (technical grade), hp-β-CD (average M_W approximately 1,540 g mol^{-1}), and rhodamine B (approximately 95% pure) were purchased from Sigma–Aldrich. β-E2 (>99% pure) was purchased from Alfa Aesar. Sodium iodide (NaI, analytical grade) and sodium sulfate decahydrate (>98% pure) were purchased from Nacalai Tesque (Japan). Sodium dihydrogen phosphate (>99.0% pure) from Kishida Kagaku (Japan) and disodium hydrogen phosphate (>99.5% pure) from Kanto Kagaku (Japan) were purchased to prepare a phosphate-buffered solution (20 mM, pH 7.0). All sample solutions were made with purified water through a Millipore filter (Milli-Q Laboratory, Nihon Millipore, Japan, resistivity 18.2 MΩ cm).

Preparation of $(HTA)_2SO_4$

In the cyclic voltammetry, we used dihexadecyltrimethylammonium sulfate $(HTA)_2SO_4$ instead of HTAB because the bromide (Br^-) disturbs voltammograms. HTAB was dissolved in ethanol and 1.2 eq. silver sulfate was added to precipitate out the Br^- as silver bromide crystal. The silver bromide was removed from the solution with the filtration. Then, the ethanol solution of $(HTA)_2SO_4$ was evaporated and the dry salt was solubilized in methanol. The solubilized salt was recrystallized with acetone twice. The final crystals were filtered and dried in a vacuum desiccator.

Methods

Interfacial tension (γ) measurement

Two types of interfacial tensiometer were used. One was a pendant drop interfacial tensiometer (Model PD-X assisted with FAMAS version 1.7.0 software, Kyowa Interface Science, Japan). A drop of sample was suspended from an 18-gauge stainless steel needle. The water jacket around the drop was thermostated at 25.0±0.1 °C by a circulating water bath (Model RTE-5, Neslab, US). All data were recorded more than 5 min after the drop formation. A Du Nong-type interfacial tensiometer (Model AquaPi & EZ-Pi, Kibron, Finland) was also used. This tensiometer was placed in the box where the humidity was kept high and the water temperature was 24 °C. All data were recorded after the reading became constant. These instruments were calibrated with pure water. All measurements were performed after 1 h equilibrium.

Fluorescence anisotropy measurement

All the fluorescence anisotropy measurements were performed on a BEACON 2000 spectrometer (Pan Vera) at 25.0±0.1 °C. This apparatus is equipped with a 100-W halogen lamp as an excitation source and a thermostated cell housing chamber which is fitted with a circulating water bath to control temperature. Rhodamine B (RB) was used as a fluorescence probe [10]. Fluorescence anisotropy was measured by using excitation and emission wavelengths of 570 and 630 nm, respectively. The size of both emission and excitation slits were 10 nm. The concentration of RB was kept at 0.1 μM. RB is expected to solubilize in the surface region of micelles and report the information about microstructural changes in there. The degree of depolarization of the fluorescence emission of a molecule probe is a measure of its rotational diffusion during the excited lifetime. The steady-state anisotropy (r) is related to the viscosity around the probe by Perrin's equation:

$$\frac{r_0}{r} = 1 + \frac{kT\tau}{V\eta} \tag{1}$$

where r_0 is the limiting value of emission anisotropy obtained in the absence of rotational freedom, τ is the average lifetime of the fluorophore excited state, T is the absolute temperature, k is the Boltzmann constant, V is the effective molecular volume of the probe, and η is the viscosity around the probe. From Perrin's equation, it is clear that a larger anisotropy corresponds to a more rigid environment at a fixed temperature. The obtained polarization value (P) was converted to the r value by the following equation:

$$r = \frac{2P}{3 - P} \tag{2}$$

The anisotropy values of the probe RB in micelle medium are taken as the average value of 10 readings.

DLS

For dynamic light scattering (DLS) measurements, the High Performance Particle Sizer (Model HPPS, Malvern, UK)

was used. The excitation source was He–Ne laser light of 633 nm. The scattering angle was chosen at 173° in order to reduce the multiple scattering. A disposable plastic cuvette with 1-cm path length was used for each measurement. The temperature was kept at 25.00±0.01 °C. All data were recorded 10 min after the setting of the cuvette and as the cumulus of ten times measurements. The hydrodynamic radius (R_H) of micelle values was taken as the average value of three readings.

Cyclic voltammetry measurement

The electrode reaction of I_2/I^- was studied in micellar solutions. A platinum disk electrode (BAS, φ=1.6 mm) as a working electrode, a silver–silver chloride electrode as a reference electrode, and a platinum wire as a counter electrode were used. Each scan was performed after the working electrode was polished with aluminum powder (0.3 μm) and rinsed with pure water. All sample solutions contain 0.49 M sodium sulfate and 0.01 M sulfuric acid as supporting electrolytes. The differential potentiostat (Model HECS-310B, Huso, Japan) was used. The concentration of sodium iodide was constant at 0.5 mM. Each scan was performed at 10 mV s^{-1}. The cyclic voltammograms (CVs) of sodium iodide solution containing hp-β-CD in the absence and in the presence of a 10-min argon aeration were recorded. The influence of the dissolved oxygen on the CV was not observed (figure not shown). Therefore, all of the CVs were performed under no pretreatment of Argon aeration.

Results and discussion

Interfacial tension of NP solution at different hp-β-CD concentrations

The interfacial tension (γ) of the NP solution at different hp-β-CD concentrations is plotted in Fig. 1. The interfacial tension decreases with the increase of the NP at any hp-β-CD concentration. Hp-β-CD is constituted of seven glucose units and forms a ring which has a hydrophilic outer surface and a hydrophobic inner cavity and well known to incorporate guest molecules in the hydrophobic cavity predominantly in a 1:1 stoichiometry [11]. In aqueous solution of hp-β-CD, NP is considered to incorporate the hydrophobic cavity of hp-β-CD. Hp-β-CD is well known not to adsorb at the air–solution interface because of its hydrophilic outer surface. It indicates that the NP molecules which are not incorporated in the hp-β-CD cavity adsorb at the air–solution interface. The break point which demonstrates the onset of micellization (i.e., critical micelle concentration (cmc)) has not been observed at any hp-β-CD concentration. Because NP is very hydrophobic, the NP

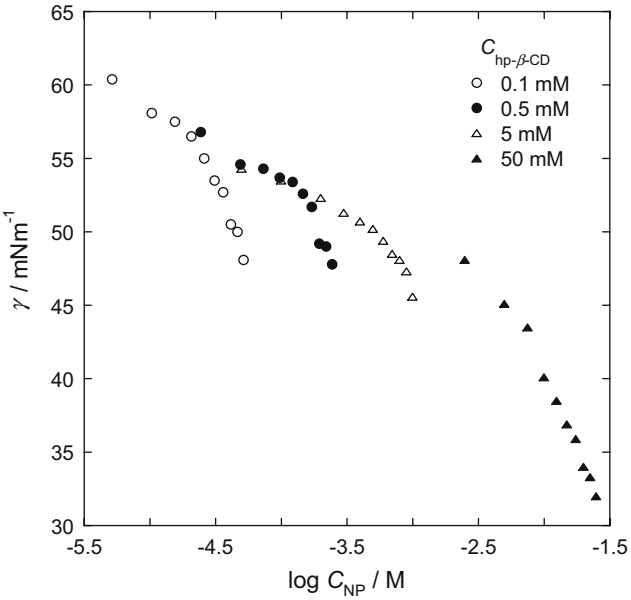

Fig. 1 Interfacial tension (γ) vs. log C_{NP}/mol dm^{-3} at various hp-β-CD concentrations

monomer concentration in the bulk phase cannot increase up to the cmc. From γ vs. log C_S, the maximum surface excess (Γ_{max}) of nonionic NP was estimated by Gibb's adsorption equation as follows [12]:

$$\Gamma_{max} = -\frac{\lim_{C_s \to cmc}\left(\frac{d\gamma}{d\log C_s}\right)}{2.303RT} \quad (3)$$

where C_S and R are the NP concentration and gas constant, respectively. The surface excess values are listed in Table 1. The surface excess values were nearly constant at any hp-β-CD concentration and had the average value of 4.6 μmol m^{-2}. It means that hp-β-CD does not influence the orientation of the NP molecules adsorbed at the air–solution interface. In comparison to the surface excess value of HTAB (3.9 μmol m^{-2}) [6], NP seems to occupy a lesser area per molecule than HTAB at the air–solution interface. The electrostatic repulsive force between the head groups of HTAB and the volume of the three methyl groups in hydrophilic portion of HTAB inhibits the crowded packing.

Table 1 The surface excess (Γ_{max}) values of the NP at different concentrations of hp-β-CD

$C_{hp\text{-}\beta\text{-}CD}$/mM	Γ_{max}/μmol m^{-2}
0.1	4.9_2
0.5	4.2_9
5	4.7_4
50	4.3_6
	4.6[a]

[a] Average

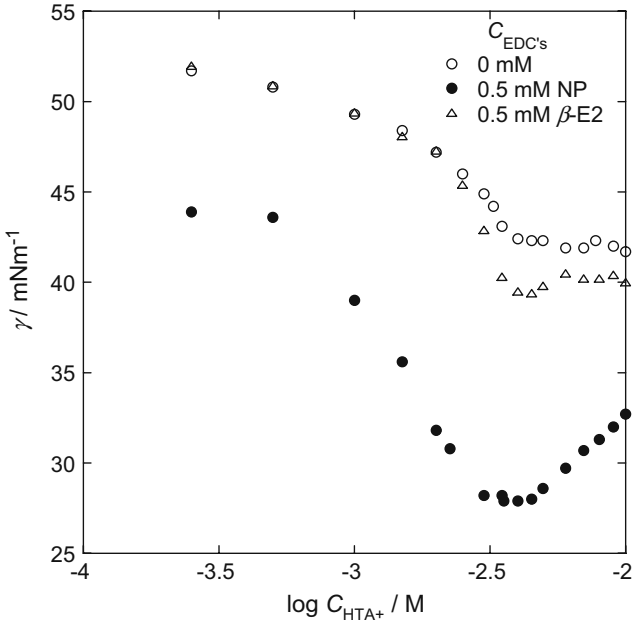

Fig. 2 Interfacial tension (γ) vs. log C_{HTA}^{+}/mol dm^{-3} in the presence of each endocrine disruptors: 5 mM hp-β-CD, 0.49 M Na_2SO_4, and 0.01 M H_2SO_4

Interfacial tension of HTA^+ solution with hp-β-CD and sulfate ion

To investigate the influence of the supporting electrolyte on the adsorptive property of HTA^+ at the air–solution interface, we measured interfacial tension of the HTA^+ solution containing sulfate ion. The interfacial tension of the HTA^+ solution containing sulfate ion is plotted in Fig. 2. The cmc and maximum surface excess values of HTA^+ ion are listed in Table 2. The surface excess value of HTA^+ in the presence of a swamping amount of supporting electrolyte was estimated by Eq. (3) where C_S is the HTA^+ concentration. These cmc values are much larger than the cmc value of HTAB aqueous solution in the absence of hp-β-CD and sulfate ion (0.92 mM) [6]. This means that HTA^+ ion is incorporated inside the hp-β-CD cavity and the concentration of HTA^+-free monomer decreases. We have observed the decrease in cmc value of HTA^+ in the presence of both EDCs. We can explain this decrease of cmc with the two possible reasons. The first one is the stabilization of micelle by EDCs. It is due to the attractive interaction between the hydroxyl groups and the τ electrons of aromatic rings in NP or β-E2 and the positively charged ammonium portion in HTA^+ ion. It reduces the electrostatic repulsion between the polar head groups of HTA^+ in the micelle [13]. Moreover, the hydrophobic interaction between NP or β-E2 and HTAB micelle stabilizes the micellization [14]. The second one is that both EDC molecules occupy the hp-β-CD cavity and increase the concentration of HTA^+-free monomer. However, NP decreased the cmc values more significantly than those of β-E2. From the viewpoint of molecular structure, NP has a long carbon chain in itself and is similar to HTA^+ ion. It makes a higher affinity between HTA^+ and NP in micelle formation and increases the concentration of HTA^+-free monomer more significantly. Although the maximum surface excess value of HTAB in the presence of β-E2 is larger than that value in the presence of NP, the interfacial tension of the latter EDC is very much lower than that of the former EDC. In the NP solution, the NP molecules are also adsorbed at the air–solution interface, which also works to lower the interfacial tension. However, above the cmc, as the C_{HTAB} and the micelle concentration increase, the adsorbed NP molecules desorb from the air–solution interface and are distributed in micelle and the composition of NP at the interface decreases. Therefore, the interfacial tension largely goes up again.

Table 2 The cmc and surface excess (Γ_{max}) values of the HTA^+ solution at different NP or β-E2 concentrations in the presence of 5 mM hp-β-CD containing 0.49 M Na_2SO_4 and 0.01 M H_2SO_4

C_{EDCs}	cmc/mM	Γ_{max}/μmol m^{-2}
0 mM	3.9_5	4.5_9
0.5 mM NP	3.0_6	3.4_0
0.5 mM β-E2	3.5_0	7.7_3

Fluorescence anisotropy

The more rigidly the RB molecule is solubilized in the surface region of micelle, the larger the r value is [15]. The change in r value is shown in Fig. 3. At 0.1 mM, the r value decreased. It indicates that the beginning of solubilization of EDCs into micelle disturbs the close packing of RB molecule at the micelle surface. As the concentration of NP increased, the r value increased. However, as the concentration of β-E2 increased, the r value once recovered and seemed to decrease little by little. It indicates that the solubilization of NP makes the micelle surface more rigid but the solubilization of β-E2 does not. NP is more similar to HTA^+ in structure. Therefore, NP solubilizes between the ionic heads of HTA^+ in micelle, reduces the electrostatic repulsion of the ionic heads at the micelle surface, and makes the micelle more stable and rigid [16]. On the other hand, β-E2 seems to disturb the orientation of HTA^+ and lessen the rigidity of micelle surface.

DLS

We investigated the R_H of HTA^+ micelle by dynamic light scattering method in the presence of each EDC (Fig. 4) [17]. As the concentration of EDCs increases, the hydrodynamic radius of micelle seems to increase little by little.

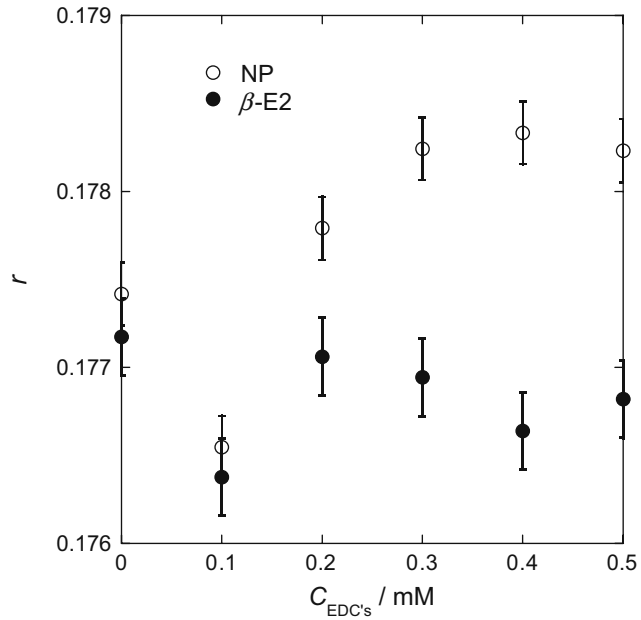

Fig. 3 Fluorescence anisotropy (r) value vs. C_{EDCs}/mM: 50 mM hp-β-CD, 20 mM HTAB, 0.49 M Na_2SO_4, and 0.01 M H_2SO_4

This trend was similar in both EDCs. In our pyrene fluorescence I_1/I_3 experiments, the polarity in the micelle did not change by the addition of each EDC (data not shown). Hence, this small increase in hydrodynamic radius is not due to the invasion of water molecule in the micelle; rather, it is due to the invasion of EDC molecules. Moreover, the invasion of EDCs at the micelle surface seems to lower the electric density at the surface and possibly increases the aggregation number.

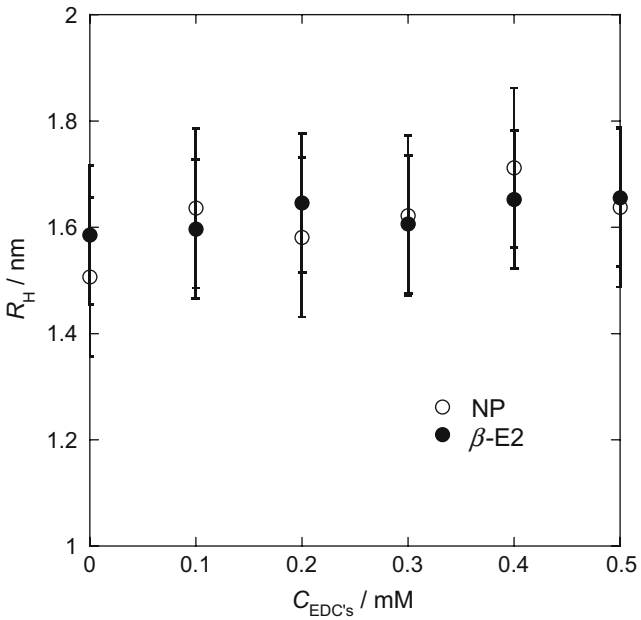

Fig. 4 R_H of micelle vs. C_{EDCs}/mM: 50 mM hp-β-CD, 20 mM HTAB, 0.49 M Na_2SO_4, and 0.01 M H_2SO_4

Cyclic voltammetry of I_2/I^- in the presence of hp-β-CD

Here, we have chosen the I_2/I^- as the electrochemical probe because the charge of I^- was expected to make its binding to cationic micelle easy, and the electroneutral I_2 was expected to solubilize between the hydrophobic portions of surfactant in micelle and to solubilize in the surfactant monolayer at the electrode surface. We investigated the influence of hp-β-CD to the redox peaks of I_2/I^- (Fig. 5). In the absence of hp-β-CD, an anodic peak of I^- at about 530 mV and a cathodic peak of I_2 at around 480 mV were observed. In the presence of 50 mM hp-β-CD, both anodic and cathodic peak currents decreased and their peak potentials shifted to the negative direction. The decrease of the anodic peak current is caused by the binding of I^- with the hydrophilic surface of hp-β-CD. On the other hand, the decrease of the cathodic peak current is caused by the inclusion of I_2 in the hydrophobic cavity of hp-β-CD [18]. The negative shift of the peak potentials indicates that the I_2 incorporated in the hp-β-CD cavity was more stabilized than the I^- bonding to the surface of hp-β-CD.

Cyclic voltammetry of I_2/I^- in the presence of HTA^+ ion and hp-β-CD

We have also investigated the influence of HTA^+ cation (Fig. 6). The cmc of HTA^+ ion from interfacial tension measurement in the same composition with the solution of

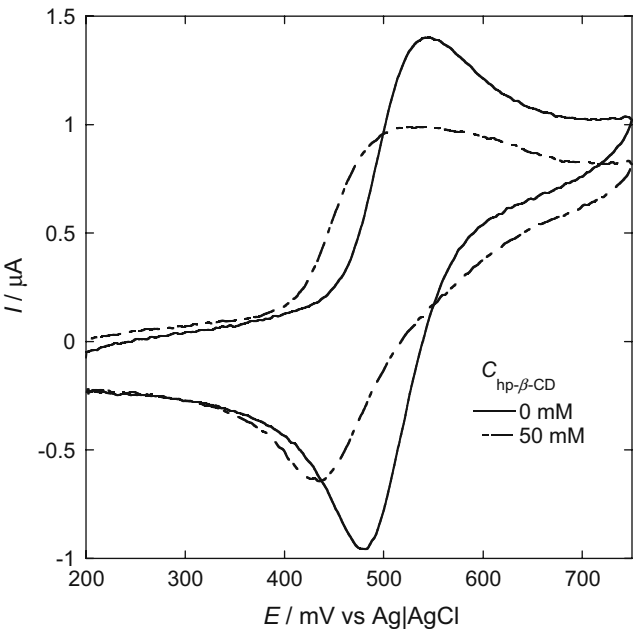

Fig. 5 Cyclic voltammogram of I_2/I^- in the presence of 5 mM hp-β-CD and in the absence of hp-β-CD: 0.5 mM NaI, 0.49 M Na_2SO_4, 0.01 M H_2SO_4

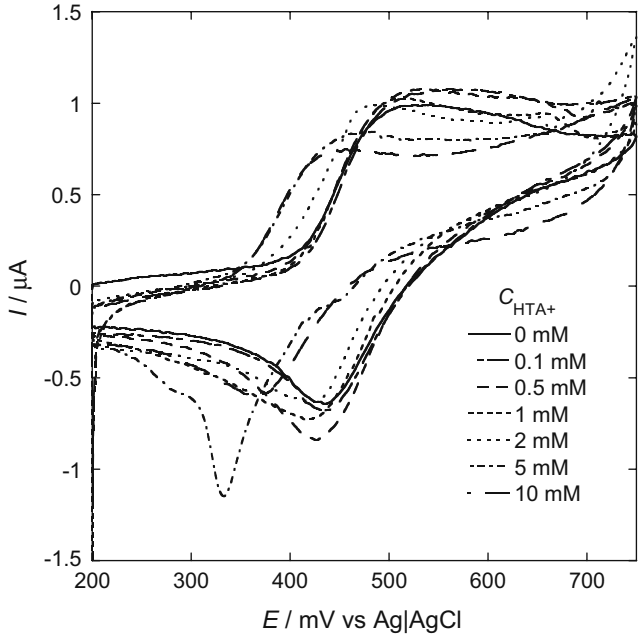

Fig. 6 Cyclic voltammogram of I_2/I^- at various HTA^+ ion concentrations: 0.5 mM NaI, 5 mM hp-β-CD, 0.49 M Na_2SO_4, 0.01 M H_2SO_4

CV measurements stated in the caption of Fig. 6 was 3.9_5 mM. Both the anodic and cathodic peaks of I_2/I^- are higher than those in the absence of HTA^+. The increase of the anodic and cathodic peak currents is due to the release of trapped I^- and I_2 from the hp-β-CD into the bulk, which is caused by the replacement of I^- and I_2 in the hp-β-CD cavity with HTA^+. On the other hand, as the concentration of HTA^+ increases above the cmc, both the anodic and cathodic peak currents become lower than those at the premicellar concentration. Before the I_2 and I^- bonding to the micelle experience electron transfer, the micelle has to turn around so that the I_2 and I^- face against the electrode surface. It causes the decrease of peak currents. Moreover, both the anodic and cathodic peak potentials shifted to the negative direction. It indicates that the I_2 solubilized in the HTA^+ micelle was more stabilized than the I^- bonding to the surface of HTA^+ micelle. As the HTA^+ concentration increases up to 5 mM, a sharp adsorptive reduction peak was observed at 330 mV. The I_2 formed at the platinum electrode surface in the absence of any surfactant is known to adsorb at the electrode surface [19]. In our systems, the HTA^+ inhibited the adsorption of I_2 at the low HTA^+ concentration. However, as the HTA^+ concentration increased, the HTA^+ monolayer was formed, which caused the absorption of I_2 in the HTA^+ monolayer on the electrode surface. As the HTA^+ concentration increased up to 10 mM, the adsorptive reduction peak disappeared. At this concentration, the I_2 formed at the electrode surface dissolved into the HTA^+ micelle. Therefore, the adsorptive peak was not observed.

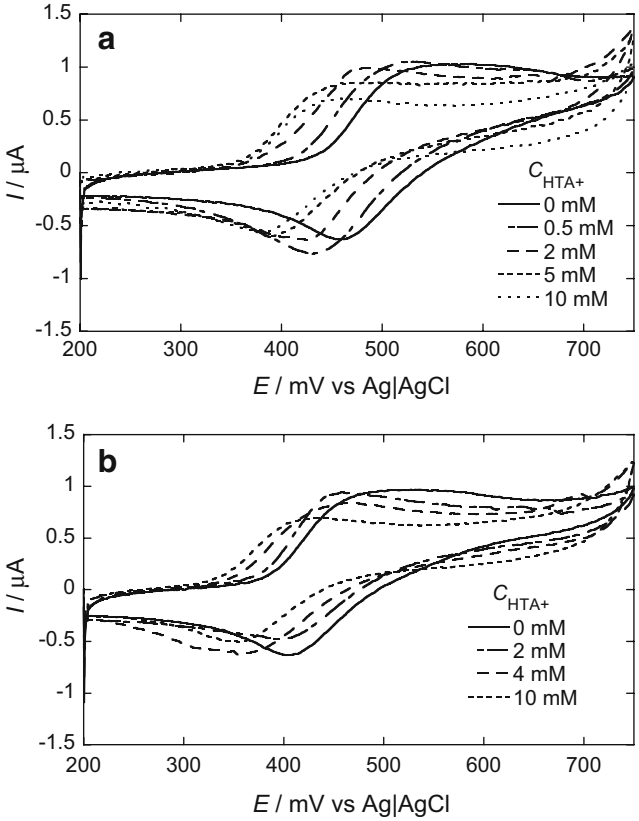

Fig. 7 Cyclic voltammogram of I_2/I^- at various HTA^+ ion concentrations in the presence of 0.5 mM NP (**a**) or 0.5 mM β-E2 (**b**): 0.5 mM NaI, 5 mM hp-β-CD, 0.49 M Na_2SO_4, 0.01 M H_2SO_4

Cyclic voltammetry of I_2/I^- in the presence of NP or β-E2, HTA^+, and hp-β-CD

The cyclic voltammograms of I_2/I^- in the systems containing NP or β-E2 are shown in Fig. 7a and b, respectively. The cmc of HTA^+ of the respective systems were 3.0_6 and 3.5_0 mM from the interfacial tension measurement and listed in Table 3. The peak potential shifted to the negative direction even in the premicellar concentration of HTA^+. It indicates that the I^- is solubilized in the HTA^+ monolayer formed at the electrode surface even at the low HTA^+ concentration below the cmc. In the HTA^+ monolayer, the I_2 is more stabilized than the I^-. At the postmicellar HTA^+ concentration, the negative shift of the peak potential was larger in the NP solution than in the β-E2 solution. It is because NP decreases the cmc more effectively and, in the

Table 3 The cmc values of the HTAB solution at different NP or β-E2 concentrations in the presence of 50 mM hp-β-CD containing 20 mM phosphate buffer and 0.5 μM pyrene

C_{EDCs}	cmc/mM
0 mM	4.6_1
0.5 mM NP	3.8_5
0.5 mM β-E2	4.4_7

bulk phase at the same concentration (0.5 mM) of NP or β-E2, the amount of formed micelle is larger in NP. The outstanding adsorptive reduction peak observed in Fig. 6 was not observed in Fig. 7a. However, in Fig. 7b, there was a broad adsorptive peak observed at around 340 mV at the HTA^+ concentration of 4 mM. In NP solution, the larger amount of micelle dissolved the I_2 formed at the electrode surface, carried them away from there, and reduced the adsorption peak current of I_2.

Conclusion

We investigated the interactions of EDCs such as NP and β-E2 with HTA^+ micelle and HTA^+ monolayer formed at the electrode surface via interfacial tension, fluorescence anisotropy, dynamic light scattering, and cyclic voltammetry in the presence of hp-β-CD. Hp-β-CD can be useful for the experiments using less soluble chemicals in water such as these EDCs. The solubilization of EDCs in the micelle increases the rigidity of micelle surface and the hydrodynamic radius but does not change the polar environment in the micelle. At the low HTA^+ concentration, HTA^+ works to prevent I_2 from adsorbing at the electrode surface. The HTA^+ monolayer formed at the electrode surface adsorbs I_2 in it. However, in the presence of HTA^+ micelle, the I_2 dissolves in the micelle. The cyclic voltammetry of I_2/I^- can be a very helpful tool to investigate the adsorbing condition of surfactants at the solid-solution interface. NP, which has a more similar structure to HTA^+, decreased the cmc more effectively.

Acknowledgements We are grateful to Prof. H. Tsukube and Prof. T. Nagasaki (Osaka City University, Japan) for their helpful assistance in the steady-state fluorescence, fluorescence anisotropy, and dynamic light scattering measurements. PS is grateful to Dr. R. Tanaka (Osaka City University, Japan) and also to the Japan Society for the Promotion of Science (JSPS) for postdoctoral fellowship award.

References

1. Davis DL, Bradlow HL, Wolff M, Woodruff T, Hoel DG, Anton-Culver H (1993) Environ Health Perspect 101:372
2. Colborn T, vom Saal FS, Soto AM (1993) Environ Health Perspect 101:378
3. Colborn T (1995) Environ Health Perspect 103(Suppl 7):135
4. Harrison PTC, Holmes P, Humfrey CDN (1997) Sci Total Environ 205:97
5. Kuramitz H, Natsui J, Sugawara K, Itoh S, Tanaka S (2002) Anal Chem 74:533
6. Kosaka O, Sehgal P, Doe H (2005) J Surfactants Deterg 8:347
7. Kosaka O, Sehgal P, Doe H (2008) Food Hydrocoll 22:144 DOI 10.1016/j.foodhyd.2007.01.024
8. Brix R, Hvidt S, Carlsen L (2001) Chemosphere 44:759
9. Song W, Li A, Xu X (2003) Ind Eng Chem 42:949
10. Maiti NC, Krishna MMG, Britto PJ, Periasamy N (1997) J Phys Chem B 101:11051
11. Otzen DE, Oliveberg M (2001) J Mol Biol 313:479
12. Menger FM, Galloway AL, Chlebowski ME (2005) Langmuir 21:9010
13. Hassan PA, Yakhmi JV (2000) Langmuir 16:7187
14. Chiang H, Lukton A (1975) J Phys Chem 79:1935
15. Tamura K, Nii N (1989) J Phys Chem 93:4825
16. Delacruz JL, Blanchard GJ (2003) J Phys Chem B 107:7102
17. Marchetti S, Onori G (2005) J Phys Chem B 109:3676
18. Wang Y, Mendoza S, Kaifer AE (1998) Inorg Chem 37:317
19. Osteryoung RA, Anson FC (1964) Anal Chem 36:975